Title

Selective Hydrogenation of Furan-Containing Condensation Products as a Source of Biomass-Derived Diesel Additives

Journal

ChemSusChem, 7(10)

ISSN

1864-5631

Authors

Balakrishnan, Madhesan
Sacia, Eric R
Bell, Alexis T

Publication Date

2014-10-01

DOI

10.1002/cssc.201402764

Peer reviewed

ChemPubSoc Europe

DOI: 10.1002/cssc.201402764

Selective Hydrogenation of Furan-Containing Condensation Products as a Source of Biomass-Derived Diesel Additives

Madhesan Balakrishnan, Eric R. Sacia, and Alexis T. Bell*[a]

In this study, we demonstrate that while the energy density and lubricity of the C_{15} and C_{16} products of furan condensation of biomass-derived aldehydes with 2-methylfuran are consistent with requirements for diesel, these products do not meet specifications for cetane number and pour point due to their aromatic furan rings. However, a novel class of products that fully meet or exceed most specifications for diesel can be produced by converting the furan rings in these compounds to cyclic ether moieties. Full hydrodeoxygenation of furan condensation products to alkanes would require 55–60% higher hydrogen demand, starting from biomass, compared to the products of furan ring saturation, providing an additional incentive to support the saturated products. We also report here on a tunable class of catalysts that contain Pd nanoparticles supported on ionic liquid-modified SiO_2 that can achieve complete saturation of the furan rings in yields of 95% without opening these rings.

Increasing global demand for diesel[1] and higher efficiency of diesel engines compared to gasoline engines[2] have stimulated the search for chemical pathways by which biomass can be converted into diesel. Particular attention has been focused on using lignocellulosic biomass rather than vegetable oils, since lignocellulosic biomass gives higher yields per acre and can be grown on land that is not suitable for food crops.[3] The cellulose and hemicellulose fractions of lignocellulosic biomass can be hydrolyzed to produce glucose and xylose, which can readily be dehydrated to produce 5-hydroxymethylfurfural (HMF) and furfural (FUR), respectively.[3c,4]

Prior work has shown that FUR and HMF are good starting materials for the formation of products that can be blended into conventional diesel. One approach to this end involves hydrodeoxygenation of the products of aldol condensation of furfural or HMF with acetone to produce high-value alkanes suitable as diesel additives.[5] More recently, several alternatives have emerged, including acid-catalyzed hydroxyalkylation/alkylation of biomass-derived aldehydes, such as furfural, with 2-methylfuran, a compound that can be produced by selective hydrogenation of furfural.[6] A benefit of hydroxyalkylation/alkylation, also known as furan condensation, is that it can be carried out in solvent-free conditions with up to 97% selectivity to desired products at 65 °C.[7] Moreover, the range of substrates that can undergo such reactions is very broad, enabling a variety of biomass-derived aldehydes, alcohols, and ketones (e.g., HMF, furfural, 5-methylfurfural, 5-methylfurfuryl alcohol, formaldehyde, acetone, and acrolein) to react with 2-methylfuran.[6c,7] Detailed studies demonstrating production of alkanes from a variety of these products and their boiling distribution have been reported previously.[6c]

Many products of second-generation biomass conversion processes contain oxygen and unsaturated groups, often in the form of furan rings. While these functionalities can be eliminated via hydrodeoxygenation, several recent studies have shown that high-quality diesel fuels can be formed that do not necessitate complete oxygen removal.[8] It is also notable that the cetane number of various oxygenates can be estimated using artificial neural network models, and often display good properties.[9] Molecules containing cyclic and acyclic ether moieties have been demonstrated to have particularly good combustion characteristics;[10] for example, the cetane number of ethyl tetrahydrofurfuryl ether has been reported to be 80–90, and this product reduces soot emissions by 50% in a 30% (*v*/*v*) blend with conventional diesel.[8c] However, the high volatility significantly limits its inclusion in diesel.

To produce fuels that better fit into the C_{11}–C_{22} blends of fuels typical for diesel, we propose combining the high-yield of furan condensation with selective saturation of the products to create fuels with cyclic ether functionalities, as illustrated in Scheme 1. We have reported previously that acid-catalyzed condensation of 5-methylfurfural with 2-methylfuran (2-MF) produces tris(5-methylfuran-2-yl)methane, **1**, in yields up to 97% in solvent-free conditions in the presence of a heterogeneous acid catalyst.[7] Under similar conditions, condensation of furfural with 2-MF produces 5,5′-(furan-2-ylmethylene)bis(2-methylfuran), **2**, in yields of approximately 93%.[7]

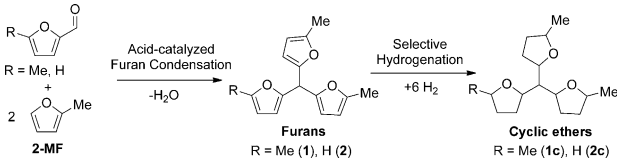

Scheme 1. Cyclic ethers formed through condensation and hydrogenation of biomass-derived furans.

[a] *Dr. M. Balakrishnan,[+] E. R. Sacia,[+] Prof. A. T. Bell*
Department of Chemical and Biomolecular Engineering
University of California, Berkeley
107 Gilman Hall, Berkeley, CA 94720 (USA)
E-mail: bell@cchem.berkeley.edu

[+] *These authors contributed equally to this work*

Supporting Information for this article is available on the WWW under http://dx.doi.org/10.1002/cssc.201402764.

Table 1. Fuel properties of furans, cycle ethers, and standard fuels.[a]

Property	Condensation product		Hydrogenation product		ULSD ref.
	1	**2**	**1c**	**2c**	
DCN	22.3	25.5	59.8	60.4	41.4[14]
T_{fp} [°C]	31	11	<-40	<-40	−18[14b]
$\nu_{40\,°C}$ [mm^2 s^{-1}]	18.1	11.8	7.33	7.45	2.30[14]
lubricity [mm]	160	160	220	180	571[14]
$\rho_{40\,°C}$ [g mL^{-1}]	1.086	1.102	0.983	1.007	0.809[15]
ΔH_{comb} [MJ L^{-1}]	35.9	35.9	35.9	35.6	33.6[8d]

[a] DCN: derived cetane number; T_{fp}: freezing point; $\nu_{40\,°C}$: kinematic viscosity at 40 °C; $\rho_{40\,°C}$: density at 40 °C; ΔH_{comb}: energy density. [b] Cloud point was used instead of freezing point since ULSD is a multicomponent mixture.

A comparison of relevant fuel properties [i.e., derived cetane number (DCN), freezing point, kinematic viscosity at 40 °C ($\nu_{40\,°C}$), lubricity, density, and energy density] determined for **1** and **2** with those found previously for ultralow sulfur diesel (ULSD) is presented in Table 1. The DCN values of **1** and **2** are well below that of ULSD while the kinematic viscosities of **1** and **2** are much higher. The high freezing points and kinematic viscosities of **1** and **2** are attributable to the aromaticity of these materials and are a consequence of π–π interactions between furan rings. However, **1** and **2** do possess high volumetric energy densities and exceptional lubricity, defined by the size of the wear scar formed when a steel ball is rubbed against a stationary disk in a pool of the test liquid under a defined load, frequency, and time (ASTM D6079). The smaller the wear scar diameter, the better lubricity. Due to increasing requirements for removal of lubricity-enhancing sulfur-containing molecules in ULSD and the poor lubricity of alkanes, molecules that can act as lubricity additives are desirable. It has been shown previously that a significant reduction in wear scar can be achieved by addition of as little as 2% of additives like fatty acid methyl ester (FAME) biodiesel, after which the benefit is substantially lessened.[11] This finding suggests that **1** and **2** could be attractive diesel additives, even at small concentrations, to enhance lubricity.

Scheme 2 illustrates the progression of products formed when **1** undergoes hydrogenation. Full saturation of the three furan rings to produce **1c** is expected to provide the best properties with the least H_2 input based on published trends in functional group properties.[8c,10] The ether functionalities in **1c** are less able to stabilize free radicals formed during combustion than the aromatic furan ring, resulting in a shorter ignition delay in the spark-free diesel engine combustion chamber and, therefore, a higher cetane number. Hydrogenolysis of **1c** to produce compounds **1d** and **1e** is not desirable because the cetane number of alcohols is lower than that of ethers[10] and alcohols have higher water solubility, thereby increasing their partitioning into groundwater if spilled.

Table 1 demonstrates that the properties of **1c** and **2c** are in general superior to those of **1** and **2**. The DCNs of **1c** and **2c** are substantially greater than those of **1** and **2**, and exceed that of ULSD by a significant margin. Due to the removal of π–π interactions, saturation of the furan rings in **1** and **2** reduces the freezing point significantly below that of ULSD, but the viscosities of **1c** and **2c**, while lower than those of **1** and **2**, still remain higher than that of typical diesel. We also note that the densities of **1c** and **2c** are 9% lower than those of **1** and **2**. However, the exceptionally high volumetric energy density of **1** and **2** is preserved in **1c** and **2c** because the chemical energy of the added H_2 goes directly into the fuel rather than being lost as water through hydrodeoxygenation. Finally, despite a reduction in viscosity, **1c** and **2c** retain their exceptional lubricity due to retention of the heteroatom, which is known to aid in lubricity.[11]

Given the superior fuel characteristics of **1c** and **2c**, efforts were undertaken to identify catalysts that could be used to hydrogenate **1** with high selectivity to **1c**. Platinum, palladium, ruthenium, and rhodium supported on carbon and Al_2O_3 were explored and the results are presented in Table 2, entries 1–8.

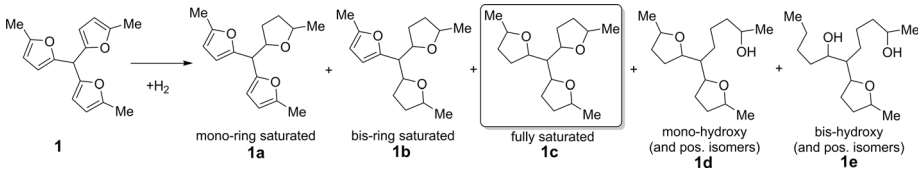

Scheme 2. Products formed on hydrogenation of **1**.

Table 2. Screening of catalysts and conditions for selective formation of **1c**.[a]

Entry	Catalyst	Loading [mol%]	Time [h]	Temp [°C]	Press. [MPa]	Conversion [%]	Yield [%]				
						1	**1a**	**1b**	**1c**	**1d**	**1e**
1	Pt/C	0.2	10	100	2.1	21	14	1	3	2	1
2	Pd/C	0.2	10	100	2.1	100	1	11	57	16	15
3	Ru/C	0.2	10	100	2.1	65	34	17	3	6	5
4	Rh/C	0.2	10	100	2.1	42	30	5	1	4	2
5	Pt/Al_2O_3	0.2	10	100	2.1	19	10	1	4	3	0
6	Pd/Al_2O_3	0.2	10	100	2.1	99	2	34	38	14	10
7	Ru/Al_2O_3	0.2	10	100	2.1	46	32	9	3	1	1
8	Rh/Al_2O_3	0.2	10	100	2.1	100	33	58	5	3	1
9	Pd/C	0.2	10	75	1.4	98	2	45	39	9	3
10	Pd/Al_2O_3	0.2	10	75	1.4	79	60	19	0	0	0
11	Pd/C	0.5	24	140	2.1	100	0	0	50	15	35
12	Pd/C	0.5	24	140	4.2	100	0	17	30	7	46

[a] Conditions: 1 g of **1** (solvent-free conditions), 500 rpm stirring. Catalyst loading: total metal content with respect to **1**.

A comparison of metal dispersions for these commercial catalysts is included in the Supporting Information. Because the dispersion of these metals supported on carbon is very similar, the intrinsic activity of the metal can be deduced from entries 1–4. Additional screening at other conditions can also be found in the Supporting Information. In order to minimize reactor volume and prevent the need for further product separation, all reactions were run under solvent-free conditions. At 100 °C and 2.1 MPa H_2 pressure, carbon- and alumina-supported palladium and rhodium catalysts showed significant activity towards the production of **1b** and **1c**. Consistent with studies of 2,5-dimethylfuran saturation to 2,5-dimethyltetrahydrofuran,[12] palladium was found to be significantly more active for complete ring saturation than platinum, rhodium, or ruthenium, but also formed significant quantities of the hydrogenolysis products, **1d** and **1e**. Hydrogenation at the milder conditions of 75 °C and 1.4 MPa of H_2 using Pd/C as the catalyst still produced significant quantities of **1d** and **1e**. As expected, raising the temperature to 140 °C and increasing reaction time (entry 11) and H_2 pressure (entry 12) also resulted in the formation of significantly more **1d** and **1e**. Introduction of solvents was also ineffective in forming **1c** selectively with carbon- and alumina-supported palladium catalysts (Supporting Information).

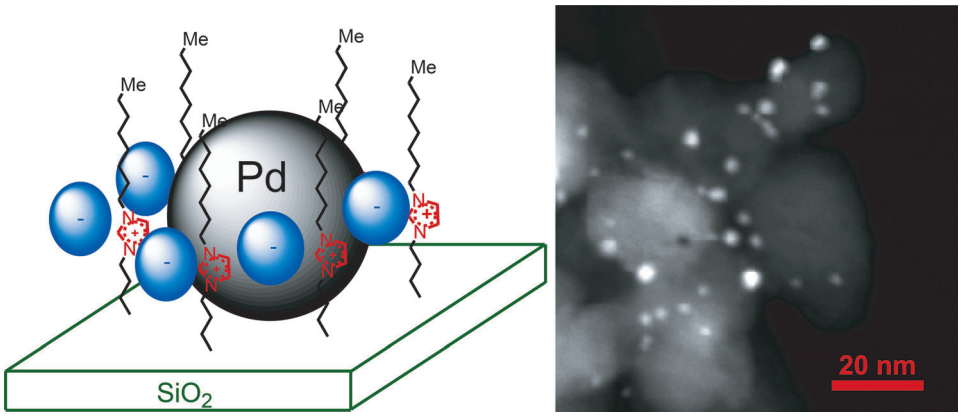

Figure 1. Diagram of surface of Pd/IL-SiO_2 and HAADF-STEM of surface of Pd/IL(PF_6^-)-SiO_2.

As an alternative to Pd/C and Pd/Al_2O_3, we next considered palladium nanoparticles formed on a surface of SiO_2-containing surface-bound ionic liquids (ILs).[13] The investigation of this class of catalysts was motivated by their reported activity and selectivity for the reduction of nitrobenzene to aniline.[13a] Moreover, ionic liquid strands tethered to a SiO_2 surface have been reported to limit agglomeration and leaching of palladium nanoparticles, thereby enhancing catalyst stability.[13] Another attractive feature of these catalysts is the tunability of the surface properties, which can be changed by altering the size, hydrophobicity, and softness of the IL anions. To examine the effectiveness of these catalysts for the selective hydrogenation of furanic fuel precursors, palladium nanoparticles were supported on the surface of 1-propyl-3-octyl imidazolium chloride tethered silica (Figure 1). The octyl functionality of the IL tether was chosen to facilitate the stability of palladium nanoparticles as well as the hydrophobicity of the surface. The loading of the IL functionality was 0.33 mmol g^{-1} (0.48 molecules nm^{-2}). To understand the role of the anion on the distribution of hydrogenation products, the Cl^- anion was exchanged after nanoparticle formation for BF_4^-, NTf_2^-, and PF_6^-. Analysis of HAADF-STEM images revealed that the average size and distribution of the palladium nanoparticles were unaffected by the composition of the anion, viz., Cl^- (2.7 ± 1.4 nm), BF_4^- (2.6 ± 1.0 nm), NTf_2^- (2.7 ± 1.2 nm), and PF_6^- (2.5 ± 1.1 nm). It is notable that the average diameters of the palladium nanoparticles (Figure 1) are comparable to the estimated spacing between the tethered IL moieties, ~2 nm, suggesting that these species help stabilize the size of the palladium nanoparticles during their synthesis.

As shown in Table 3, entries 1–4, all of these catalysts are quite active for the transformation of **1** into **1b–d**; however, only the catalyst containing PF_6^- anions, which have the right balance of hydrophobicity, size, and softness, exhibits a high selectivity for production of **1c**. As the furan rings are hydrogenated, they become more hydrophilic by the loss of aromaticity; therefore, it is hypothesized that hydrophobic PF_6^- anions reduce the retention of the product, **1c**, on the catalyst

Table 3. Screening of Pd/IL-SiO_2 for selective formation of **1c** and **2c**.[a]

Entry	IL catalyst anion	Loading [mol%]	Time [h]	Temp [°C]	Press. [MPa]	Conversion **1** [%]	Yield **1a** [%]	**1b** [%]	**1c** [%]	**1d** [%]	**1e** [%]
1	Cl^-	0.2	10	100	2.1	100	0	41	5	39	15
2	BF_4^-	0.2	10	100	2.1	100	0	62	12	15	11
3	NTf_2^-	0.2	10	100	2.1	97	9	36	1	41	11
4	PF_6^-	0.2	10	100	2.1	100	0	3	66	14	16
5	PF_6^-	0.2	5	100	2.1	100	0	2	88	8	2
6	PF_6^-	0.2	10	75	1.4	100	0	19	78	2	0
7	PF_6^-	0.2	5	75	2.1	100	0	7	91	2	0
8	PF_6^-	0.2	10	75	2.1	100	0	1	95	4	0
						Conversion **2** [%]	Yield **2a** [%]	**2b** [%]	**2c** [%]	**2d** [%]	**2e** [%]
9	PF_6^-	0.5	30	60	2.8	100	0	7	92	1	0

[a] Conditions: 1 g of **1** or **2** (solvent-free conditions), 500 rpm stirring. Catalyst loading: total metal content with respect to **1** or **2**.

surface where it could otherwise undergo hydrogenolysis to **1d** and **1e**. Investigation of the reaction temperature, time, and H_2 pressure (entries 5–8) indicates that the catalyst activity for hydrogenolysis can be reduced by working at lower temperatures. Comparison of Pd/IL(PF_6^-)-SiO_2 (entry 6) with Pd/C (Table 2, entry 9) clearly demonstrates that under identical reaction conditions, Pd/IL(PF_6^-)-SiO_2 exhibits a much higher selectivity to **1c** and limited selectivities to **1d** and **1e**. By optimizing the reaction conditions for hydrogenation over Pd/IL(PF_6^-)-SiO_2, the selectivity to the targeted product, **1c**, can be raised to 95% (entry 8). Optimized conditions were also found for reactant **2** (entry 9), resulting in a yield of 92% to **2c**. Due to reduced steric hindrance on one of the furan rings in **2**, milder temperatures and longer times were required to form this product in high yields without hydrogenolysis. The conditions leading to this optimization are given in the Supporting Information.

The Pd/IL(PF_6^-)-SiO_2 catalyst was subjected to five reaction cycles (>35000 TON) at the conditions shown for entry 8 of Table 3. The results are shown in the Supporting Information. The catalyst retained nearly all of its activity throughout all cycles for hydrogenation of **1**, but a decrease in **1c** selectivity to 84% was observed. This result also corresponded to an increase in formation of both **1b** and **1d**. HAADF-STEM imaging of spent Pd/IL(PF_6^-)-SiO_2 showed a slight particle size increase to 3.0 ± 1.7 nm (Supporting Information). Once nanoparticles grow in size so that exposed particles are significantly larger than IL strands, the beneficial surface selectivity effects may be lost, and the results will become more similar to Pd/C. Improvement may be made in the future by synthesizing a Pd/IL-SiO_2 catalyst with longer alkyl chains or a higher loading of IL strands to prevent agglomeration of nanoparticles. While the synthesis of Pd/IL-SiO_2 catalysts could be implemented at larger scales, the costs of producing such catalysts cannot be clearly established at this time.

This work shows that high yields of **1c** and **2c** can be achieved by selective hydrogenation of **1** and **2** over Pd/IL(PF_6^-)-SiO_2. It also demonstrates that **1c** and **2c** exhibit properties equivalent or superior to those of conventional diesel and, hence, could be considered as biomass-derived diesel blending agents. Finally, we note that the production of **1c** and **2c** requires 35–38% less H_2 than the production of pure hydrocarbons containing the same number of carbon atoms. This feature has implications for the environmental impact of the products **1c** and **2c**. At present, the most economical approach for H_2 generation is steam reforming of methane, a process that releases 0.25 molecules of CO_2 per molecule of H_2 produced. As a consequence, the ratio of "green" to "black" carbon atoms is 5.82 and 6.0 for the synthesis of **1c** and **2c**, respectively, whereas for the synthesis of the corresponding C_{16} and C_{15} alkanes, the ratio of "green" to "black" carbon is 3.76 and 3.75, respectively. In summary, this work demonstrates that diesel blending agents with excellent properties can be produced in high yield by selective hydrogenation of **1** and **2**, products that can be produced from biomass.

Experimental Section

Compounds **1** and **2** were synthesized using the methods discussed in the Supporting Information. The materials were characterized by GC/MS and NMR prior to use.

The following catalysts were purchased as 5 wt% metal content from Aldrich: Rh/Al_2O_3, Rh/C, Ru/Al_2O_3, Pt/Al_2O_3, and Pd/Al_2O_3. The remaining catalysts were obtained from Acros: Ru/C (5 wt%), Pt/C (5 wt%), and Pd/C (10 wt%). The synthesis of silica-supported ionic liquid catalysts with palladium (1 wt%) is described in the Supporting Information.

In a typical experiment, 1 g of starting material was added to an autoclave along with 0.2 mol% of catalyst by total metal content. The autoclave was then sealed into the HEL ChemSCAN system. The reactor was purged twice with N_2 and twice with H_2 before heating to the desired reaction temperature and then pressurizing with H_2. All reaction vessels were stirred magnetically at 500 rpm. After completion of the reaction, 0.15 g of dodecane was added as an internal standard and the mixture was transferred to a vial. The reactor was washed three times with ethyl acetate to complete the transfer of all material. The final mixture was diluted with ethyl acetate to appropriate concentrations for measurement and analyzed by a flame ionization detector attached to a Varian CP-3800 gas chromatograph.

Methods for property determination of starting materials and selective hydrogenation products are discussed in depth in the Supporting Information. DCN measurements were carried out according to ASTM D6890 at the National Renewable Energy Lab (NREL) in Golden, CO, USA. Lubricity was measured according to ASTM D6079 by Intertek Group plc. in Benicia, CA, USA.

Acknowledgements

This work was supported by the Energy Biosciences Institute. E.R.S. also acknowledges support from a National Science Foundation Graduate Research Fellowship under Grant No. DGE 1106400. The authors also acknowledge the contributions of Jon Luecke, Matthew Ratcliff, and Brad Zigler from NREL for DCN testing, Matthew Deaner for contributions to the experimental portion of this manuscript, and Sebastian Werner for assistance with the acquisition of STEM images.

Keywords: biomass · furan hydrogenation · heterogeneous catalysis · renewable fuels · sustainable chemistry

[1] OPEC, *World Oil Outlook* (Eds.: J. Griffin, A.-M. Fantini, K. Aylward-Marchant), **2013**, Vienna, Austria.
[2] L. Guzzella, A. Amstutz, *IEEE Control Syst. Mag.* **1998**, *18*, 53.
[3] a) C. Somerville, H. Youngs, C. Taylor, S. C. Davis, S. P. Long, *Science* **2010**, *329*, 790; b) J. Janaun, N. Ellis, *Renewable Sustainable Energy Rev.* **2010**, *14*, 1312; c) G. W. Huber, S. Iborra, A. Corma, *Chem. Rev.* **2006**, *106*, 4044.
[4] a) D. M. Alonso, J. Q. Bond, J. A. Dumesic, *Green Chem.* **2010**, *12*, 1493; b) A. Voll, W. Marquardt, *Biofuel Bioprod Bioref* **2012**, *6*, 292.
[5] G. W. Huber, J. N. Chheda, C. J. Barrett, J. A. Dumesic, *Science* **2005**, *308*, 1446.
[6] a) A. Corma, O. de La Torre, M. Renz, N. Villandier, *Angew. Chem. Int. Ed.* **2011**, *50*, 2375; *Angew. Chem.* **2011**, *123*, 2423; b) A. Corma, O. de La Torre, M. Renz, *ChemSusChem* **2011**, *4*, 1574; c) A. Corma, O. de La Torre, M. Renz, *Energy Environ. Sci.* **2012**, *5*, 6328.
[7] M. Balakrishnan, E. R. Sacia, A. T. Bell, *ChemSusChem* **2014**, *7*, 1078.

[8] a) M. Balakrishnan, E. R. Sacia, A. T. Bell, *Green Chem.* **2012**, *14*, 1626; b) G. Gruter, E. De Jong, *Biofuels Technol.* **2009**, *1*, 11; c) E. de Jong, T. Vijlbrief, R. Hijkoop, G.-J. M. Gruter, J. C. van der Waal, *Biomass Bioenergy* **2012**, *36*, 151; d) M. Mascal, E. B. Nikitin, *ChemSusChem* **2009**, *2*, 423; e) E. R. Sacia, M. Balakrishnan, A. T. Bell, *J. Catal.* **2014**, *313*, 70.

[9] T. Sennott, C. Gotianun, R. Serres, M. Ziabasharhagh, J. Mack, R. Dibble in *ASME 2013 Internal Combustion Engine Division Fall Technical Conference*, American Society of Mechanical Engineers, **2013**, pp. V002T02A009.

[10] M. J. Murphy, J. E. Taylor, R. L. McCormick, *Compendium of Experimental Cetane Number Data*, (Ed.: NREL), Golden, **2004**, NREL/SR-540 – 36805.

[11] K. Wadumesthrige, M. Ara, S. O. Salley, K. Y. S. Ng, *Energy Fuels* **2009**, *23*, 2229.

[12] a) M. Chatterjee, T. Ishizaka, H. Kawanami, *Green Chem.* **2014**, *16*, 1543; b) T. Thananatthanachon, T. B. Rauchfuss, *Angew. Chem. Int. Ed.* **2010**, *49*, 6616; *Angew. Chem.* **2010**, *122*, 6766.

[13] a) J. Li, X.-Y. Shi, Y.-Y. Bi, J.-F. Wei, Z.-G. Chen, *ACS Catal.* **2011**, *1*, 657; b) Y. Kume, K. Qiao, D. Tomida, C. Yokoyama, *Catal. Commun.* **2008**, *9*, 369.

[14] B. R. Moser, S. F. Vaughn, *Bioresour. Technol.* **2010**, *101*, 646.

[15] K. A. Doll, B. K. Sharma, P. A. Z. Suarez, S. Z. Erhan, *Energy Fuels* **2008**, *22*, 2061.

Received: July 29, 2014
Published online on August 28, 2014